ELSEVIER

Finite Elements in Analysis and Design 36 (2000) 83–98

FINITE ELEMENTS IN ANALYSIS AND DESIGN

www.elsevier.com/locate/finel

Failure modeling of sawn lumber with a fastener hole

Judsen M. Williams[a], Kenneth J. Fridley[b,*], William F. Cofer[b], Robert H. Falk[c]

[a] *KPFF Consulting Engineers, 2401 Colorado Ave. Suite 315, Santa Monica, CA 90404, USA*
[b] *Civil and Environmental Engineering, Washington State University, Pullman, WA 99164-2910, USA*
[c] *USDA Forest Products Laboratory, Madison, WI 53705, USA*

Abstract

There is a consistent reduction in member strength associated with long-term use of structural wood members. It is hypothesized that this reduction in strength is due to "use and aging" effects such as cracks, splits and checks developed from drying stresses, moisture cycling, and fastener holes originating from initial construction techniques. The focus of this research effort was to develop an accurate model of the behavior and performance of the recycled timbers containing fastener holes. The flexural capacity of structural wood joists and planks containing fastener holes was modeled utilizing finite element analysis (FEA) coupled with the tensor polynomial (Tsai–Wu) strength theory. Each model presented herein represents a connection detail that is commonly used in construction. To validate the analytical approach, virgin timbers with drilled holes were conditioned to simulate in situ conditions and tested to failure. Comparing the results of the analytical model to experimental behavior, the FEA results were slightly conservative with predicted strength values falling within one standard deviation from the mean value of the experimental data and thus, producing accurate results. A critical hole location exists where the hole produces the largest reduction in strength. Based on the results, it is recommended that the edge of the hole not be located within 6 mm from the extreme fiber in both the compression and tension regions. If this does occur, then possibly some post processing needs to be performed such as planing the member down such that the hole is located on the edge, or the hole is completely eliminated from the section.

Keywords: Finite element analysis; Wood; Strength reduction; Holes

1. Introduction

With the increased interest in the use of recycled materials as structural elements and components, the focus of recycling has shifted from small-scale curbside recycling to mainstream

* Corresponding author. Tel.: 509-335-7320; fax: 509-335-7632.
E-mail address: fridley@wsu.edu (K.J. Fridley).

0168-874X/00/$ - see front matter
PII: S0168-874X(00)00010-X

construction. Since the turn of the century, more than 7.3 billion cubic meters of lumber and timber have been sawn in the United States, much of it still residing in existing structures [1]. Similarly, there is a large portion of wood industrial and military buildings that were constructed during World War II that are slated for demolition. It is estimated that over 1.0 million cubic meters of lumber and timber could be reclaimed and reused from these structures [1]. Thus, with the available recycled material, there has become a need to estimate and quantify the residual strength capacity of the used materials. This is especially true for recycled structural solid wood members.

At this time, there are no standards or recommendations for structural reuse of wood. All design values and grading rules are applicable only to virgin timber. Using current design practices, engineers assume that the short-term strength of wood remains unchanged with use, assuming that the parent material is not subjected to decay or rot. However, it has long been recognized that the failure of wood is dependent on the magnitude, rate and duration of applied load. This time-dependent characteristic of wood is known as duration of load (DOL) in wood design and continues to be one the major areas of uncertainty in wood research [2].

In recent studies, researchers have observed that there is a consistent reduction in member strength associated with long-term use. It is hypothesized that this reduction in strength is due to "use and aging" effects such as cracks, splits and checks developed from drying stresses, moisture cycling, and fastener holes originating from initial construction techniques. Therefore, a comprehensive research project was developed between Washington State University, the US Forest Products Laboratory (FPL) in Madison, Wis., the West Coast Lumber Inspection Bureau (WCLIB), and the Clean Washington Center to investigate the flexural capacity of structural joists and planks containing fastener holes. Finite element analysis (FEA) coupled with the tensor polynomial (Tsai–Wu) strength theory was utilized to analytically predict the effect of the fastener hole. The finite element models were developed to model the behavior and performance of the recycled timbers containing fastener holes. Each model represents a connection detail that is commonly used in construction. Investigating the effect of a fastener hole is the first step in assessing the structural capability and marketability of recycled timbers.

Complementing the analytical models presented herein, an experimental program was developed to calibrate and validate the analytical model. All experimental testing was organized and performed at the FPL. The test setup, material species and dimensions used in the experimental program were identical to the analytical tests. Initially, actual recycled material was to be used for the experimental testing. However, due to economics, availability and sample size considerations, virgin timbers were obtained, had holes drilled in them, and conditioned to simulate in-situ conditions.

The overall objective of this research was to develop and calibrate an analytical model that can accurately predict the ultimate failure capacity of recycled wood members containing fastener holes. Comparisons are made between various hole configurations to determine possible critical locations and hole sizes. The specific objectives are to: (1) develop an analytical model that can be used for further prediction of strength for recycled wood members; (2) investigate the accuracy of the Tsai–Wu failure theory as a predictive tool of the ultimate flexural capacity of wood beams; and (3) investigate the effect of a single fastener hole on the flexural capacity of a wood beam. The results of this study are intended to provide an engineering database that can be used to establish grading criteria and appropriate design values for recycled timber.

2. Background

Despite extensive research estimating the failure of solid sawn wood beams, there has been little research to investigate the failure capacity of recycled wood members. To develop a valid and robust model, however, previous research related to the use of failure criteria for wood and the strength prediction of wood coupled with FEA are reviewed.

2.1. Strength theory applied to failure of wood

In order to analytically predict the ultimate failure strength of each specimen, a tensor polynomial (Tsai–Wu) strength theory for anisotropic materials was utilized. The Tsai–Wu yield criterion is an operationally simple theory that is based on a scalar function of two strength tensors [3]. Originally developed to predict the failure of filamentary composite materials, the strength theory has several advantageous attributes that differ from other existing failure criteria. Specifically, all of the invariant requirements of coordinate transformations are satisfied. The general form for anisotropic materials can be specialized to account for different material symmetries including orthotropic materials. This takes into account differences between tensile and compressive strength and accounts for multi-axial states of stress.

The general form of the failure surface proposed by Tsai and Wu [3] has the scalar form:

$$F_i\sigma_i + F_{ij}\sigma_i\sigma_j = 1 \quad \text{for } i,j = 1,2,\ldots,6, \tag{1}$$

where F_i and F_{ij} are strength tensors of the second and fourth rank, respectively, and σ_i and σ_j are the related applied stresses for three dimensions.

Derived from the general form of Eq. (1), the specialized case for an orthotropic material such as wood becomes

$$F_1\sigma_1 + F_2\sigma_2 + F_{11}\sigma_1^2 + 2F_{12}\sigma_1\sigma_2 + F_{22}\sigma_2^2 + F_{66}\sigma_6^2 = 1 \tag{2}$$

for the plane-stress state for which $\sigma_1 = \sigma_{11}$, $\sigma_2 = \sigma_{22}$, $\sigma_6 = \tau_{12}$, and $\sigma_3 = \tau_{13} = \tau_{23} = 0$. Furthermore, the l-direction is the perpendicular to grain orientation and the 2-direction is parallel to grain. Note that failure is defined as the point at which the value of the scalar Tsai–Wu coefficient reaches or exceeds 1.0. Liu [4] determined that the Tsai–Wu theory is reasonably accurate when used to predict failure in solid sawn wood under combined states of stress. This is found to be true when the normal stress interaction term, F_{12}, is based on the Hankinson formulas under the plane stress conditions. Similarly, Hasebe and Usuki [5] successfully used the Tsai–Wu strength theory to determine mechanical properties of Japanese cedar. Assuming that the stress perpendicular to grain is negligible, Eq. (2) was modified to a plane stress condition for which the ultimate tensile, compressive and shearing strength values were investigated. More recently, Patton-Mallory et al. [6] reviewed various research efforts and recommended that the maximum stress and Tsai–Wu failure criteria be used for wood.

2.2. Strength prediction of wood and failure modeling

Combining techniques of FEA and a strength theory to predict the ultimate load capacity has proven to be a valuable tool for both solid sawn wood and wood composites. Leichti and Tang [7]

successfully developed a plane stress, linear elastic model that predicted the ultimate load capacity of wood composite I-beams with the use of FEA and the Tsai–Wu strength theory. Using a stepwise technique in which the applied load was increased incrementally, the model was able to predict the ultimate load capacity with different web materials and web joint configurations, while identifying "weak" regions and locating areas of high-stress concentrations that led to failure.

Similarly, Cramer and Goodman [8] developed a FEA model that predicted the ultimate tensile strength of solid lumber containing circular knots and cross grain. The objective of the study was to determine the effect of knot location on the resulting stress field under a uniformly applied tension stress, parallel to the long axis of the member [8]. Using the stepwise analysis technique, the researchers were able to predict the location of the initial failure based upon a maximum stress theory. Failure was assumed to occur when the maximum tensile stress in the parallel- or perpendicular-to-grain direction exceeded the clear wood strength value. Also, Cramer and Goodman [S] utilized an "effective section technique" to model ultimate failure as a progressive series of initial failures. It was assumed that, upon initial failure, a crack would form and propagate along the grain to the end of the modeled segment. In addition, to account for the failed section of the member, the region below the knot was assumed to be ineffective in resisting any load. Therefore, a net effective section was used in the subsequent analysis. This process was used both for knots located near the edge and knots near the center. Cramer and Goodman [8] determined that the stepwise analysis was in good agreement with experimental data and that knots located near the edge of the member caused the largest longitudinal stress concentrations. Of the entire set of knot locations considered, knots near the edge, but completely encased in the member, caused the highest stress concentrations. Conversely, the lowest stress concentration occurred when the knot was located along the center of the member. Similarly, Cramer and Goodman [9] developed a finite element/fracture mechanics algorithm that predicted the ultimate tensile capacity of solid lumber with knots located within the wide face of the member. The objective of that research was to model the progressive fracture process of failure in wood members and to quantify the strength-reducing effects of knots located within the wide face of the member.

3. Modeling procedures

3.1. Member configurations

Seven member configurations were modeled (see Table 1). Each model was based on a No. 2 Coastal Douglas-fir Larch member with a cross section of 89 mm × 185 mm. Also, each model was chosen to represent a connection configuration that is common to standard construction techniques. For the purpose of this research, the fastener hole was located at the midspan of the beam to represent the connection pattern that would create the greatest section reduction relative to flexural resistance. The fastener hole sizes considered were 25.4 mm and 44.5 mm in diameter. The 25.4-mm hole represents the largest allowable bolt diameter [10] whereas the 44.5-mm hole represents half of the largest allowable edge knot on the wide face of a No. 2 structural joist and plank [11].

Although each hole configuration is located along the midspan of the member, the distance from the tension and compression faces was varied. Table 1 outlines the hole size and location used for

Table 1
Description of each member configuration with hole size and location

Case	Description
Control	Clear wood with no bolt hole
Case 1	25.4 mm bolt hole with center 38.1 mm from compression edge (see Note 1)
Case 2	25.4 mm bolt hole with center 38.1 mm from tension edge (see Note 1)
Case 3	25.4 mm bolt hole with center 19 mm from tension edge (see Note 2)
Case 4	25.4 mm bolt hole with center 12.7 mm from edge (see Note 3)
Case 5	44.5 mm bolt hole with center 47.6 mm from compression edge (see Note 1)
Case 6	44.5 mm bolt hole with center 47.6 mm from tension edge (see Note 1)
Note 1:	Edge of hole is 25.4 mm from edge.
Note 2:	Edge of hole is 6.3 mm from edge.
Note 3:	Case 4 is a half-circle notch on the tension edge.

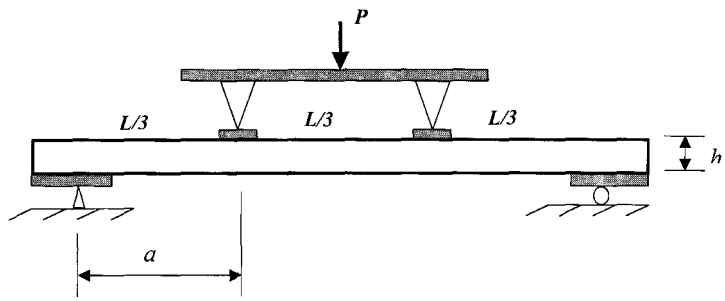

Fig. 1. Four-point (third-point loading) test setup.

each case. The location of the fastener hole is varied to investigate its effect on the ultimate flexural capacity of member. It is hypothesized that the effect on behavior of varying the location of the holes could be similar to that of knots and the edge distance requirements for knots in grading and strength ratio calculations.

3.2. Test setup

The four-point bending test, Fig. 1, was used for each specimen. The test configuration was followed as per the guidelines set forth by the American Society of Testing and Materials, ASTM D198 [12]. Each 89 mm × 185 mm specimen was 3.65 m long with a 3.35 m clear span. The shear span-to-depth ratio was $a/h = 6.1$, well within the allowable range of $a/h = 5–12$ [12]. Note that a is the distance from the support to the nearest point load and h is the depth of the beam. At the supports, 12.7 mm × 152.4 mm rigid steel bearing plates were constrained by a simply supported, pin-roller foundation. The load heads were applied at the third-points along the length of the beam.

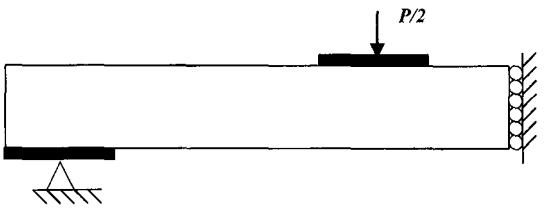

Fig. 2. Symmetrical four-point test setup.

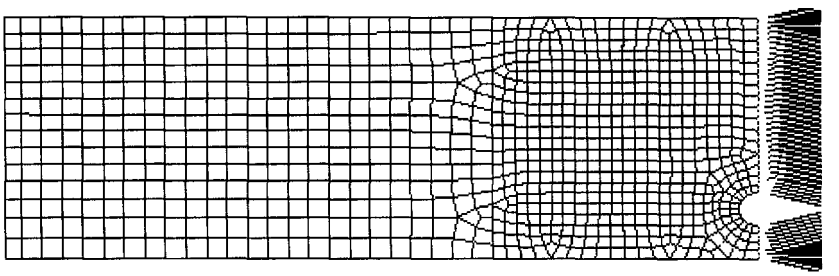

Fig. 3. Typical finite element mesh for Case 2.

3.3. Model generation

Because all loads and displacements were in-plane and the members were relatively thin with free edges, two-dimensional plane stress assumptions were applied for simplicity. All analyses were performed with ABAQUS®. When each analytical model was generated, the symmetry of the member and loading was utilized. A concentrated load was applied at the third point along the length of the beam while boundary conditions were applied to each node located along the midspan to constrain the member in the longitudinal direction. Likewise, a boundary condition was applied at the support to constrain the member in the vertical direction as illustrated in Fig. 2.

As a result of the presence of a fastener hole, there is a discontinuity in the stress flow. Therefore, localized stress concentrations form around the outer edges of the hole. To increase the accuracy of results, each mesh was generated with a fine region around the hole and coarser meshes radiating outwards towards the support as shown in Fig. 3.

3.4. Elements

All models consisted of eight-node biquadratic plane stress elements. Due to the nature of the curved surface around the hole and the radiating mesh, the eight-node elements were particularly appropriate. The isoparametric formulation makes it possible to generate elements that are nonrectangular and have curved sides. These shapes have obvious uses in grading a mesh from coarse to fine and in modeling curved boundaries [13]. To evaluate stiffness for each element, numerical integration is performed using Guass quadrature. Nine sampling points are considered within each element.

3.5. Material properties

Material properties for seasoned (dry) Douglas-fir larch (coastal) wood were obtained from the *Wood Handbook* [14]. All analyses were completed with the properties given as follows:

$$E_L = 13.4 \times 10^9 \text{ Pa}, \quad G_{LT} = 1.05 \times 10^9 \text{ Pa}, \quad \nu_{LT} = 0.45,$$

$$E_R = 0.8 \times 10^9 \text{ Pa}, \quad G_{LR} = 0.0, \quad \nu_{LR} = 0.0,$$

$$E_T = 0.8 \times 10^9 \text{ Pa}, \quad G_{RT} = 0.0, \quad \nu_{RT} = 0.0.$$

The values of E_T and E_R are computed as the average of the published modulus of elasticity (MOE) values in the tangential (T) and radial (R) directions, respectively. Also, note that the magnitude of G_{LR}, G_{RT}, ν_{LR} and ν_{RT} are taken as zero due to the plane stress configuration of the analytical model.

Failure stress limits for Douglas-fir were also obtained from the *Wood Handbook* [14] as follows:

$$\sigma_{Lt} = 85.5 \times 10^6 \text{ Pa}, \quad \sigma_{Rt} = 2.3 \times 10^6 \text{ Pa}, \quad \tau_{12} = 7.8 \text{ x } 10^6 \text{ Pa},$$

$$\sigma_{Lc} = 49.8 \times 10^6 \text{ Pa}, \quad \sigma_{Rc} = 5.5 \times 10^6 \text{ Pa},$$

where σ_{Lt} is the ultimate tensile stress in the longitudinal direction; σ_{Lc} the ultimate compressive stress in the longitudinal direction; σ_{Pt} the ultimate tensile stress in the radial direction, σ_{Rc} the ultimate compressive stress in the radial direction; and τ_{12} the ultimate shear stress in the longitudinal–radial direction. Components of the strength tensors, F_i and F_{ij}, are obtained from the failure stress limits. However, the strength interaction coefficient, F_{12}, must be determined separately. Several approaches have been used to specify F_{12} [4], the simplest of which is to use off-axis uniaxial tests. In lieu of tests, however, the author notes that $F_{12} = 0$ yields adequate results, which was used for the analyses described here.

3.6. Initial models

None of the initial analyses completed on ABAQUS® utilized any means of incrementing load. Hence, results obtained from the original analyses provided strength or capacity values for the entire member that were based on a limit defined as the initial failure at any point of stress concentration. Comparing the results to the experimental results showed that the initial method was too conservative to accurately model the actual response.

3.7. Failure prediction

In order to predict analytically the ultimate flexural capacity of each specimen, a “load-stepping’’ method was utilized in which elements that were deemed to have “failed” were removed. Inherent in this technique is the underlying assumption that the failure process was assumed to occur incrementally, as a progressive series of small, localized failures. Utilizing the principle of super-position, this method approximately modeled the propagation of cracks and load redistribution throughout the member during a loading event.

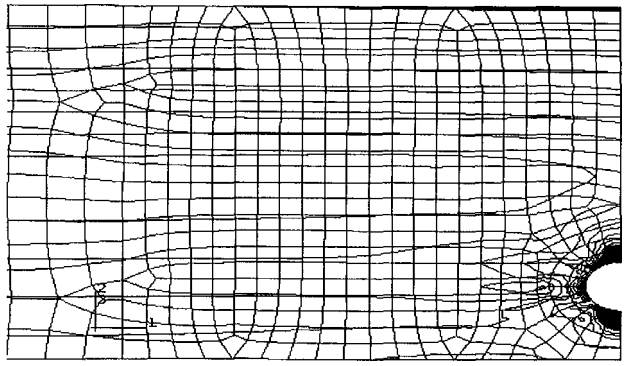

Fig. 4. Typical initial model with no elements removed.

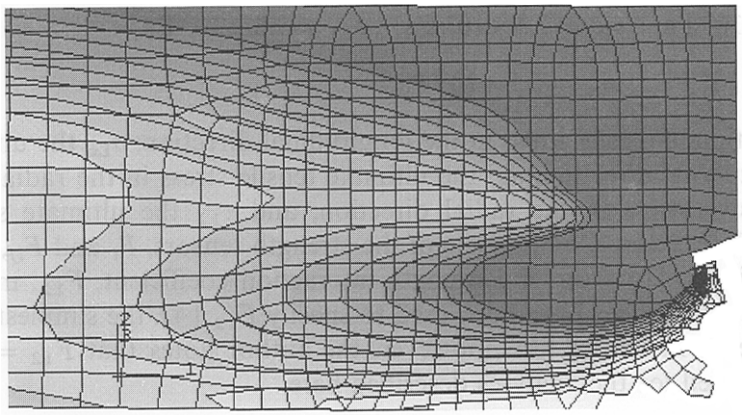

Fig. 5. Typical "effective section" after element removal.

The complete analysis was then a multi-step process. Each "step" included generating a finite element mesh and then analyzing the behavior of the model when subjected to a specific magnitude of load. The initial model was analyzed to determine the load capacity at which material failure within any element would initiate when no elements are removed (see Fig. 4).

A visual inspection of the model was performed to determine where the intensified stress regions were located. Failure of an element was defined as the point at which *all* nine integration points in an element exceeded the failure coefficient of 1.0, as defined by the Tsai–Wu failure theory [3]. Thus, when one or more elements failed, that portion of the model was removed from the mesh to create a resultant "net effective section". The net effective section was then used in the subsequent analysis step (see Fig. 5). The maximum load that produced the initial failure response was assumed to be the linear response. Responses beyond this point, in which elements were removed, were considered to be the non-linear response. The "load stepping" method was repeated until entire failure of the member occurred or the deflections became excessive.

3.8. Experimental comparisons

In order to ensure the accuracy of the values produced by the analytical model, experimental tests were performed to calibrate and validate the analytical model. All tests were organized and performed at the Forest Products Laboratory in cooperation with the G.R. Plume Co., the West Coast Lumber Inspection Bureau and Washington State University [15]. The test setup and materials were identical to the setup and materials assumed for the models in the analytical tests.

Initially, actual recycled material was to be used for the experimental testing. However, due to economics, availability and sample size considerations, virgin timbers were obtained and conditioned to simulate in situ conditions. Holes were drilled to model the actual condition of a reclaimed or recycled member. The same seven test configurations used in the analytical tests were also used in the experimental tests.

A sample size of 22 beams for each configuration was used in the experimental program, with all timbers conditioned to an average moisture content of 19%. Ultimate load, load–deflection, and mode of failure data were recorded for each specimen for comparison to analytical predictions [15].

3.9. Model verification

Using the load-stepping method as described earlier, load–deflection curves were plotted to determine the response of the model. Similarly, the US Forest Products Laboratory provided experimental load–deflection curves. Therefore, to verify that a similar response exists between the testing results and the FEA, a set of experimental load–deflection curves for a specific case was plotted with an analytical load–deflection curve on the same axis. If the load capacity and deflection response is similar throughout the loading event, then it is assumed that the numerical model accurately predicts the response.

The capacity of the recycled timbers may be conveniently reported as a "strength ratio" (*SR*) in this paper. A *SR* is derived as the ratio of moment-carrying capacity of a member with cross section reduced by the largest fastener hole to the moment-carrying capacity of the member without the defect. Thus, a member with a $SR = 0.80$ is considered to have only 80% of its original (without a hole) capacity. This procedure is identical to the approach used to publish strength ratios in ASTM D245-93, "Establishing Structural Grades and Related Allowable Properties for Visually Graded Lumber" [16]. The *SR* provides an accurate and efficient method of assessing the change in capacity when a defect such as a fastener hole is present. For the purpose of this research, the SR provided a measure of the relative effect the different hole configurations have on the flexural capacity.

4. Results and discussion

One of the main goals of this research project is to develop an analytical model that could successfully and accurately predict the ultimate flexural capacity of recycled, or pseudo-recycled,

Table 2
Strength ratio of numerical and experimental results[a]

Case	Maximum load (kN)				Number of standard deviations from mean
	Analytical	Experimental (n = 22)			
		Mean	Standard deviation	Coefficient of variation	
Control	44.8	44.2	11.2	0.25	0.1
Case 1	36.5	39.7	10.1	0.26	– 0.3
Case 2	35.6	39.1	6.6	0.17	– 0.5
Case 3	26.7	32.9	8.7	0.27	– 0.7
Case 4	26.7	35.6	8.0	0.22	– 1.1
Case 5	32.0	35.7	6.8	0.19	– 0.5
Case 6	35.6	37.5	6.7	0.18	– 0.3

[a]See Table 1 for case description.

101 mm × 203 mm No. 2 Douglas-fir. To accomplish this, finite element models were developed using the finite element software ABAQUS®.

4.1. Strength prediction

The maximum load obtained from the analyses was based upon the ultimate load that indicated total failure of the model. The experimental value was the mean of the measured failure load. The corresponding standard deviation and coefficient of variation (COV) was calculated for the entire population of the sample set. Both analytical and experimental values are listed in Table 2. Comparing the maximum loads obtained from the FEA to the mean of the experimental tests shows that the FEA model was conservative in its prediction of the failure capacity versus the experimental data. However, for all cases but one the analytical value was within one standard deviation of the experimental mean value. Assuming a normal distribution, one standard deviation from the mean equates to approximately a 16% exclusion level, or that approximately 68% of the experimental observations fall within plus or minus one standard deviation from the mean. A positive value in Table 2 represents an analytical value that was larger than the experimental mean; conversely, a negative value corresponds to a value lower than the experimental mean.

Comparing the different hole configurations, failure in Cases 2, 3 and 5 were all very similar. Localized stress concentration developed at the top and bottom of each hole due to the discontinuity in the stress flow around the hole. Therefore, once the stress concentrations became large enough that the section of the member failed (i.e., the Tsai–Wucoefficient exceeded 1.0), the load redistributed away from the hole. This redistribution of stress is represented in a similar fashion in Figs. 4 and 5. Although the contours are actually the distribution of the Tsai–Wucoefficient, they correspond to the response of the member. Similar failure modes were observed in the experimental test specimens. To further validate the FEA model, the trends of the maximum loads between the analytical tests are similar to those reported in the experimental tests.

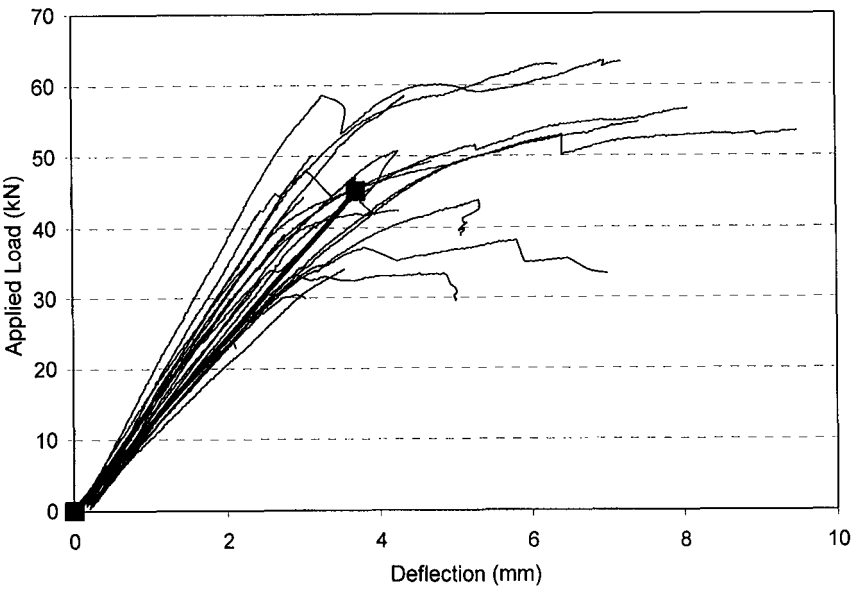

Fig. 6. Experimental and analytical load–deflection curves for the control scenario (no hole).

The lowest reduction in capacity is seen in Cases 1, 2 and 6. Cases 1 and 2 were with 25.4 mm holes centered 38 mm from the compression and tension edges, respectively. Case 6 was with a 44.5 mm hole centered 47.6 mm from the tension edge. In all three cases, the edge of the hole was located 25.4 mm from the edge of the beam. Case 5 was with a 44.5 mm hole centered 47.6 mm from the compression edge and resulted in a slightly greater reduction in capacity than Case 6. Cases 1 and 2 resulted in similar reductions in capacity, with Case 2 resulting in a slightly greater reduction than Case 1. However, Case 5 resulted in a significantly greater reduction in capacity than Case 6. Therefore, it may be concluded that the 25.4 mm holes had similar, or slightly greater, effect when located in the tension zone versus the compression zone, while the 44.5 mm holes have greater effect when located in the compression zone than when located in the tension zone.

Cases 3 and 4 resulted in similar levels of reduction in capacity. These two cases were both with 25.4 mm holes, however the edge of the hole in Case 3 was 6.4 mm from the tension edge and the center of the hole in Case 4 coincided with the tension edge (i.e., a half-hole notch resulted on the tension face). Therefore, it may be concluded that a hole very near the edge has similar effect to a hole off the edge (i.e., a circular notch). Specifically, Case 3 produced significant initial local failures. Once failure initiated around the hole and the stress concentrations redistributed around the hole, the small 6.35 mm strip of material between the edge of the hole and extreme fiber failed first. Once this portion of the member was no longer carrying load and essentially was removed from the member, along with the hole itself, the initial section becomes an “effective section” to carry the remaining the remaining load. This behavior provides evidence that a critical region, or maximum allowable region should be defined within which a hole should not be located.

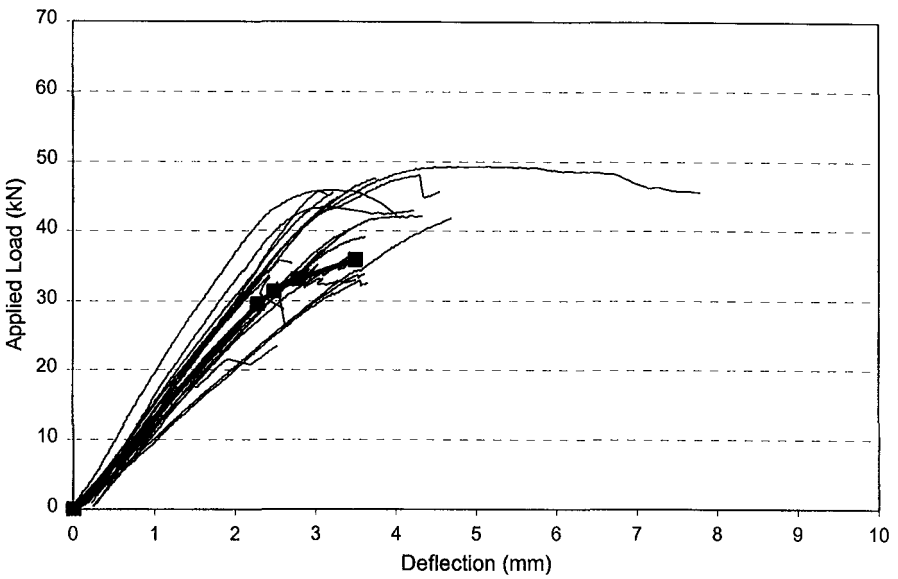

Fig. 7. Experimental and analytical load–deflection curves for Case 2.

4.2. Load–deflectionprediction

The main goal of the load-stepping technique is not only to predict accurate failure capacities, but also to attempt to model the member behavior during a loading event. Therefore, with the finite element results, load–deflection curves were plotted to compare the behavior of the model with the load-deflection curves provided by the FPL. Figs. 6–8 are plots of the load–deflection curves obtained from the finite element analyses along with the load–deflection data obtained from the entire sample of specimens tested for each respective case.

Fig. 6 is the plot of the control model, or member with no hole. It should be noted that for this configuration the load-stepping technique was unnecessary because stress concentrations did not affect the results. Failure was based on one run, with an applied unit load and failure defined with the Tsai–Wu coefficient. The initial failure of the model was the total failure load. Comparing the failure load of the control model to the models containing a fastener hole indicates the direct reduction effect on the member flexural capacity. In each case containing a hole, the failure initiated at the hole. Plus, the control model was assumed to exhibit pure elastic behavior up to failure; thus, non-linear effects were not included in the control model.

Figs. 7 and 8 are load–deflection curves for Cases 2 and 6, respectively. Both cases contain fastener holes with the edge of the hole 25.4 mm from the tension edge, but Case 2 considers a 25.4 mm hole and Case 6 considers a 44.5 mm hole. Both cases were modeled using the load-steping technique to model the nonlinear behavior. As can be seen in Figs. 7 and 8, the FEA results fall well within the spread of the experimental data, although the predicted response shifts towards the conservative edge when modeling the nonlinear region. Overall, however, the response of the model was similar to the experimental response.

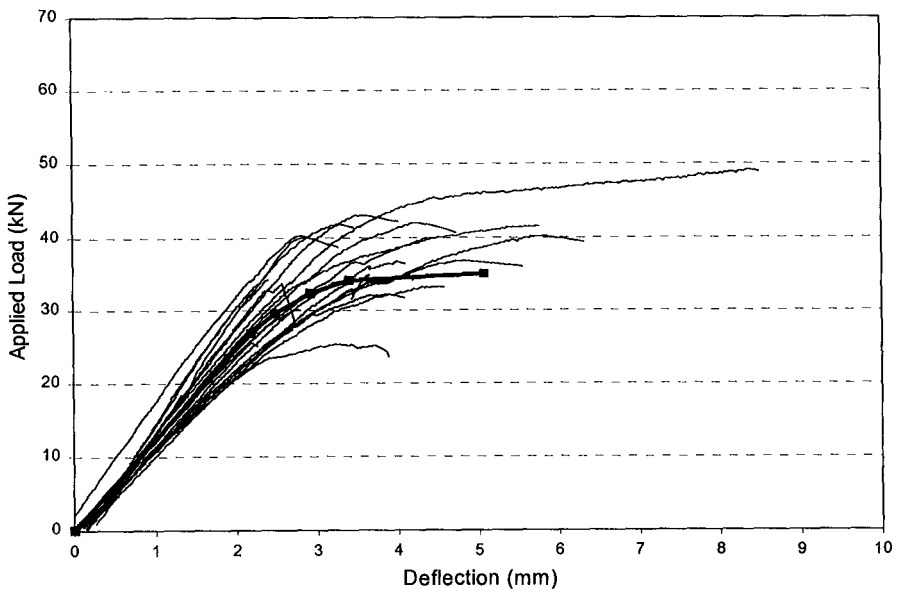

Fig. 8. Experimental and analytical load–deflection curves for Case 6.

The model-predicted failures always initiated at the hole, which is the location of the highest stress concentration. In the cases for which the hole was located within the tension region, localized stress concentrations developed at the top and bottom of each hole. When the hole was within the compression region, failure initiated at the top of the hole. This is similar to what was observed during the experimental testing as well. The Tsai–Wu coefficient was very accurate and useful for prediction of failure. However, with the nature of the equation accounting for multi-axial states of the stress and the multiple terms, it is difficult to determine which, if any, of the material properties was governing the failure. As is evident in Fig. 9, stress concentrations developed around the top and bottom of the hole, indicating the initial points of failure. It is noted that, due to the nature of the grain in the longitudinal direction, which follows the inherent stress flow around the top and bottom of a naturally occurring defect such as a knot, a relatively "smooth" flow of stress occurs around the defect. However, with an artificial defect such as a fastener hole, the flow of the grain is disrupted, thus creating an abrupt end to the wood fibers and forces the stress path around the ends of the hole. Therefore, a very high stress concentration is created. With this stress concentration, the stress flow can be thought of as a vector resultant, distributing up and over the top of the hole at some angle of inclination. If the resultant were resolved into its components, the vertical component would be creating a tension perpendicular to the grain situation. The tension-perpendicular to grain scenario is very critical in wood since the tension-perpendicular value, σ_{RT}, is approximately 40 times less than the tension-parallel (σ_{RT}) to grain allowable stress value. Thus, it is noted that the initiating failure stress is the tension-perpendicular value, σ_{RT}, caused by the hole, and it is this stress component that dominates to Tsai–Wu failure theory.

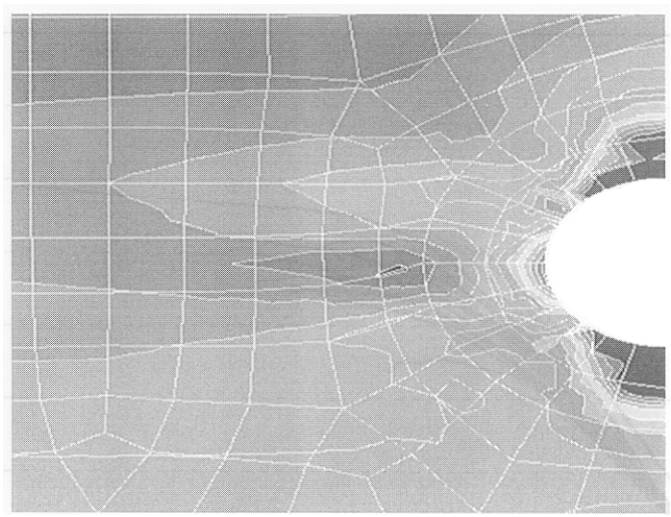

Fig. 9. Typical contour map of the distribution of Tsai–Wu coefficients.

4.3. Strength ratios

A deterministic "strength ratio" (*SR*) was obtained from the analytical tests for both the 25.4 mm and 44.5 mm hole sizes by simply dividing the moment capacity of a member with a hole by the control (no hole) moment capacity. A plot was developed to graphically describe the relationship of the hole location to the *SR* (see Fig. 10). Some additional analyses were conducted to create Fig. 10 by varying the location of the hole through the depth. As can be seen in Fig. 10, as the hole location moves away from the neutral axis of the member, the *SR* decreases or, in other words, the capacity of the parent member decreases. Intuitively, this behavior is reasonable due to the combination of the hole creating a reduction in the section modulus along with the magnitude of the applied bending stresses increasing toward the extreme fibers.

Best-fit curves were plotted over the data points to describe a relationship between the hole location and corresponding strength ratios. Again, the 44.5 mm hole creates a larger reduction than that of the 25.4 mm hole. In addition, although it appears that Fig. 10 is symmetrical, this graph corresponds with the data in Table 2 showing that slightly larger reductions for the 25.4 mm hole are in the tension region (below neutral axis) while the compression region is more critical for the 44.5 mm hole. Also, the trend of the lines for both cases is such that the *SR* decreases as the hole location goes toward the extreme fibers, but increases as the hole moves off the edge of the member and becomes a "notch". A critical hole location is therefore indicated in Fig. 10 as the minimum SR, which occurs with the edge of the hole at approximately 6 mm from the edge of the member. Thus, this is further evidence of a critical location for the hole that produces the largest strength and section modulus reduction.

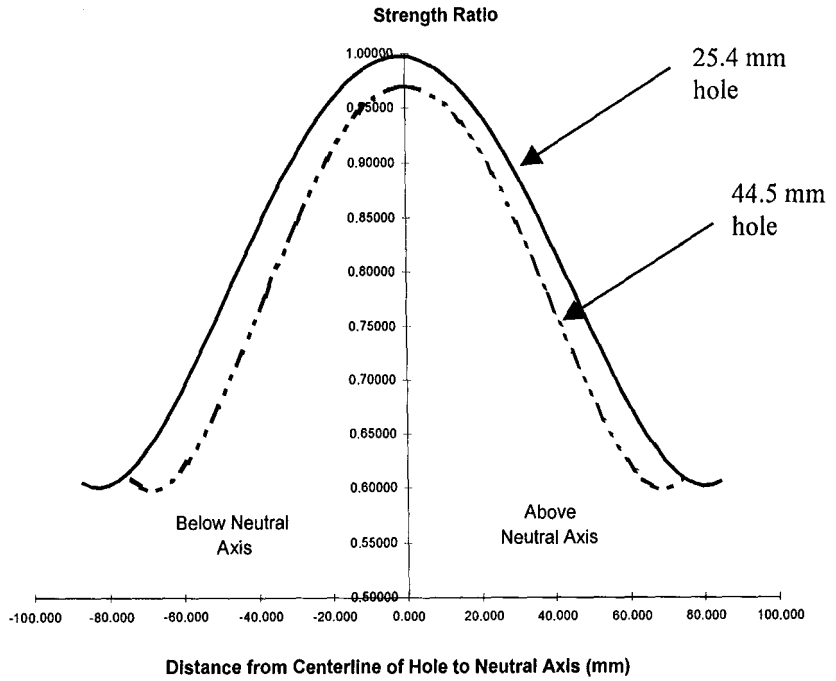

Fig. 10. Graph of the strength ratios vs. hole size and location.

5. Conclusions and recommendations

In summary, the numerical model predicted load–deflection behavior that was very similar to that of the experimental data. This was evident from the fact that each of the FEA strength predictions were within one standard deviation of the mean of the experimental failure load, and the load–deflection curves from the numerical tests fell well within was spread of the experimental load–deflection data. The model was able to accurately provide an estimate of the ultimate flexural capacity with the presence of a fastener hole.

Based upon the results of this research, several conclusions can be made:

- The presence of a hole decreases the flexural capacity of a wood member, and utilizing the Tsai–Wu failure theory as a predictive tool for determining the failure load of an orthotropic material such as wood, provides accurate strength predictions.
- Comparing the results of the analytical model to the experimental behavior, the FEA results were slightly conservative with predicted strength values falling within one standard deviation of the mean value of the experimental data, thus indicating acceptable results.
- The governing failure mode around the hole is initiated by exceeding the ultimate tension-perpendicular-to-grain stress. This ultimate value is approximately 40 times less than the ultimate tension-parallel-to-grain value.
- A critical hole location exists at which the hole produces the largest reduction in strength. Based on the results as plotted in Fig. 10, it is recommended that the edge of a 24.5 mm to 44.5 mm hole

not be located within 6 mm from to the extreme fiber in either the compression and tension regions.

References

[1] R. Falk, Wood recycling: opportunities for the wood-waste resource, Forest Products J. 47 (6) (1997) 17–22.
[2] K. Fridley, M. Hunt, J. Senft, Historical review of duration of load concepts, Forest Products J. 45 (4) (1995) 72–74.
[3] S. Tsai, E. Wu, A general theory of strength for anisotropic materials, J. Compos. Mater. 5 (1971) 58–80.
[4] J. Liu, Evaluation of the tensor polynomial strength theory for wood, J. Compos. Mater. 18 (1984) 216–226.
[5] K. Hasebe, S. Usuki, Application of orthotropic failure criterion to wood, J. Eng. Mech. 115 (4) (1987) 867–872.
[6] M. Patton-Mallory, P.J. Pellicane, F.W. Smith, Model bolted connections in wood: review, J. Struct. Eng. 123 (8) (1997) 1054–1062.
[7] R. Leichti, R. Tang, Predicting the load capacity of wood composite I-beams using the tensor polynomial strength theory, Wood Sci. Technol. 23 (1989) 109–121.
[8] S. Cramer, J. Goodman, Model for stress analysis and strength prediction of lumber, Wood Fiber Sci. 15 (4) (1983) 338–349.
[9] S. Cramer, J. Goodman, Failure modeling: a basis for strength prediction of lumber, Wood Sci. Technol. 30 (1) (1986) 189–199.
[10] American Forest and Paper Association (AF and PA), National Design Specification for Wood Construction, Washington DC, 1997.
[11] West Coast Lumber Inspection Bureau (WCLIB), Grading Rules for West Coast Lumber, Portland, OR, 1995.
[12] American Society for Testing and Materials (ASTM), D-198: Standard Methods of Static Tests of Timbers in Structural Sizes, Philadelphia, PA, 1998.
[13] R.D. Cook, D.S. Malkus, M.E., Plesha, Concepts and Applications of Finite Element Analysis, 3rd Edition, Wiley, New York, 1989.
[14] United States Department of Agriculture (USDA), Wood Handbook - Wood as an Engineering Material, USDA Forest Service, Forest Products Laboratory, Madison, WI, 1998.
[15] R.H. Falk, D. DeVisser, K.J. Fridley, Developing a grade stamp for recycled timber, Final Report to the Clean Washington Center, Seattle, WA. 1999, 34 pp.
[16] American Society for Testing and Materials (ASTM), D-245: Standard Practice for Establishing Structural Grades and Related Properties for Visually Graded Lumber, Philadelphia, PA, 1998.